Efficient laser wakefield accelerator in pump depletion dominated bubble regime

V. Horný [1,*] P. G. Bleotu [1] D. Ursescu [1] V. Malka [1,2] and P. Tomassini [1]

[1] *Extreme Light Infrastructure - Nuclear Physics, Strada Reactorului 30, RO-077125 Magurele, Romania*

[2] *Department of Physics of Complex Systems, Weizmann Institute of Science, Rehovot 7610001, Israel*

(Received 17 June 2024; accepted 1 August 2024; published 6 September 2024)

With the usage of the postcompression technique, few-cycle joule-class laser pulses are nowadays available extending the state of the art of 100 TW-class laser working at 10 Hz repetition. In this Letter, we explore the potential of wakefield acceleration when driven with such pulses. The numerical modeling predicts that 50% of the laser pulse energy can be transferred into electrons with energy above 15 MeV, and with charge exceeding several nanocoulombs for the electrons at hundreds of MeV energy. In such a regime, the laser pulse depletes its energy to plasma rapidly driving a strong cavitated wakefield. The self-steepening effect induces a continuous prolongation of a bubble resulting in a massive continuous self-injection that explains the extremely high charge of the beam rending this approach suitable for promoting Bremsstrahlung emitter and generator of tertiary particles, including neutrons released through photonuclear reactions.

DOI: 10.1103/PhysRevE.110.035202

Laser Wakefield acceleration (LWFA) of electrons [1] has opened up new opportunities for the generation of high-energy electron bunches and their application in various scientific [2,3], medical [4], and industrial [5] domains. While the mainstream of the current LWFA research lies in the generation of high-quality beams, either in the sense of high energy [6,7], low energy spread [8,9], or low emittance [10,11], there are particular applications where those parameters are of lower importance. These include the exploitation of LWFA electrons as a source of radiation and secondary particles and tertiary particles where the conversion efficiency of the laser pulse energy into the electron bunch and its total charge is crucial.

The LWFA experiments have been mainly conducted with available laser pulses of full width at half maximum duration $\tau_l \gtrsim 25$ fs. The laser focusing is matched with the plasma density to secure the smooth laser pulse guiding over many Rayleigh lengths, as the natural diffraction of the focused beam is compensated by relativistic self-focusing. The matching condition reads $k_p w_0 = 2\sqrt{a_0}$ (for $a_0 > 2$) [12] where $k_p = \omega_p/c, \omega_p = \sqrt{\frac{n_e e^2}{m_e \epsilon_0}}$ is the plasma frequency and n_e is the electron density, w_0 is the laser waist size, and $a_0 = 0.855\sqrt{I_{18}}\lambda_{l,\mu m}$ is the laser strength parameter, I_{18} is the laser peak intensity in units of 10^{18} W cm^{-2}, and $\lambda_{l,\mu m}$ is λ_l; the laser wavelength is in microns. After a given distance of propagation of the laser in the plasma, the acceleration of trapped electrons ends. This occurs either when the laser pulse energy is too depleted or even in the case the electrons overtake the accelerating part of the bubble. The propagation distances on which those occur scale as $L_{pd} \simeq \frac{1}{k_p}\frac{\omega_l^2}{\omega_p^2}\omega_p\tau_l$ and $L_d \simeq \frac{1}{k_p}\frac{4}{3}\frac{\omega_l^2}{\omega_p^2}\sqrt{a_0}$, respectively (for $a_0 > 1$). While the former linearly scales with the pulse duration, the latter only weakly depends on the intensity.

In the bubble regime [13–15], nC-class beams were predicted [16] and demonstrated [17,18] with a transverse self-injection mechanism. A possible increase of the trapped charge has been proposed by exploiting controlled injection schemes such as ionization [19] or density shock injection [20,21]. An alternative suggestion recommends exploiting near-critical-density plasma, substituting the standard bubble with a laser bubble as a 3D electromagnetic electrostatic soliton [22].

In this Letter, we discuss on available laser parameter space, with a few-cycle, joule-class laser pulses, and its benefit in the context of LWFA with the generation of nC-class electron bunches at energies in the order of hundreds of MeV. Such pulses are generated through the thin film compression (TFC) technique [23,24], providing an inexpensive and efficient shortcut to the upgrade of TW into PW-class laser systems without further amplification stages. The TFC method was successfully demonstrated at the 100 TW peak power level laser systems [25–29], while the demonstration at the 1 PW level is anticipated [29,30]. The recent experimental results [31] showing an efficient pulse duration compression ratio of a 1.5 J laser down to 6 fs show the maturity of the approach that motivates the present research.

In this range of parameters, thanks to its short duration, the laser pulse depletes the energy to plasma rapidly. Still, up to the depletion point, the pulse is intense enough to drive a strong plasma wave in a fully cavitated wakefield regime. The combination of both effects causes significant relativistic self-steepening [32,33] resulting in a strong relativistic self-focusing of a pulse which initially might be but necessarily does not have to be matched to the plasma density.

*Contact author: vojtech.horny@eli-np.ro

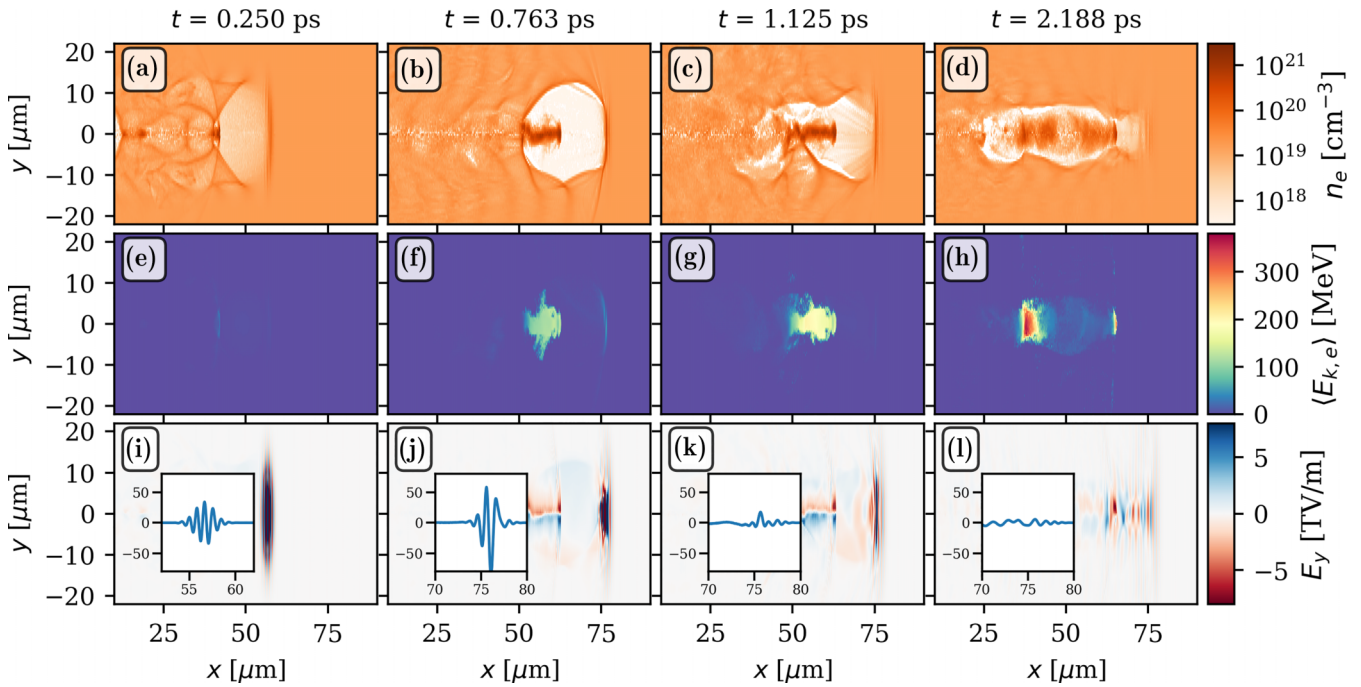

FIG. 1. Evolution of electron density n_e (a)–(d), their average energy $\langle E_{k,e} \rangle$ (e)–(h), and the electric field E_y (i)–(l).

Consequently, the bubble length continuously increases, resulting in massive continuous self-injection.

A set of numerical simulations of the electron acceleration has been conducted employing the SMILEI code [34] in the quasi-3D geometry with the decomposition into four azimuthal modes. The fundamental numerical parameters are the following. The grid resolution is always 0.25 $c\omega_l^{-1}$ and 1 $c\omega_l^{-1}$ in the longitudinal and radial direction, respectively. The integration timestep is $0.22\,\omega_l^{-1}$. The simulation box length L_x and width L_r are always set in such a way that the former is as large as at least three plasma wave periods and the latter is at least four times the laser waist size.

Plasma is represented only by electron macroparticles which are initially cold and randomly initialized within the cell. The number of macroparticles per cell is 20 and 6 in the inner and outer volumes separated by the position $r = 0.7L_r$, respectively. At the left boundary, there is a 2 μm-long vacuum followed by a 8 μm of linear density ramp to avoid unintended nonphysical effects at the boundary. The pulse is focused to $x_f = 10\,\mu$m and enters the box at $t_s = 60$ fs. The potential effects of carrier-envelope phase variations (CEP) of the pulse were anticipated [35], however, here for pulse longer than 6 fs, its influence on the pulse and bubble shape evolution, as well as the final electron spectra, is proved to be negligible. They always last at least till the peak of the laser pulse energy conversion to electrons has been achieved. The list of presented simulations and their numerical parameters is given in the Supplemental Material [36].

As an illustrative example, a case with a laser pulse of $E_{l,0} = 1.5$ J and $\tau_l = 6$ fs being initially focused to a waist of $w_0 = 10\,\mu$m leading to $a_0 = 8.57$ is chosen. The plasma density is of a quasimatched value of 1.71×10^{19} cm^{-3} ($\frac{k_p w_0}{2\sqrt{a_0}} = 1.33$). Figure 1 details the dynamic evolution of key parameters, including electron density, average electron kinetic energy within a cell, and the electric field along the polarization direction. This visualization unfolds across four distinct temporal snapshots: the onset of self-injection into the nonlinear bubble ($t = 0.25$ ps), the zenith of peak laser intensity ($t = 0.76$ ps), the pivotal time points of $t_e = 1.12$ ps when the maximum laser-to-electrons $E_e/E_{l,0}$ and $t_m = 2.19$ ps when the peak electron energy are achieved, respectively. The displayed region is confined to the central segment of the simulation box. Following the formation of the bubble, a sequence of events transpires—the relativistic self-focusing occurs, propelling the continuous longitudinal expansion of the bubble and initiating substantial, sustained continuous self-injection. In the insets in the bottom row, the value of the E_y at the laser axis around the laser pulse peak location is shown, illustrating the processes of self-steepening and pump depletion. The simulation showcases a hybrid regime of LWFA and plasma wakefield acceleration (PWFA) [37].

The acceleration process is further analyzed in Fig. 2. Panel (a) shows the energy balance within the simulation box during the acceleration; the green and brown curves show the energy stored in electromagnetic fields and as kinetic energy of simulation particles, respectively, and the blue curve is their sum. The initial swift decrease of the electromagnetic energy is caused by its rapid transfer to the wake wave and consequently to the kinetic energy of electrons.

Panel (b) illustrates the evolution of the parameter $I_{\max}$ primarily representing the laser pulse intensity that has an initial value of 1.5×10^{20} W cm^{-2}. Following the laser pulse ingress into the simulation box ($t = 60$ fs), its intensity, thanks to the relativistic self-focusing effect, rapidly increases and reaches 9.6×10^{20} W cm^{-2} at $t = 760$ fs. Over the following 350 fs, the laser pulse energy is essentially absorbed by the plasma.

Comparing panels (a) and (b), it can be observed that the maximum kinetic energy stored in all the electrons within the

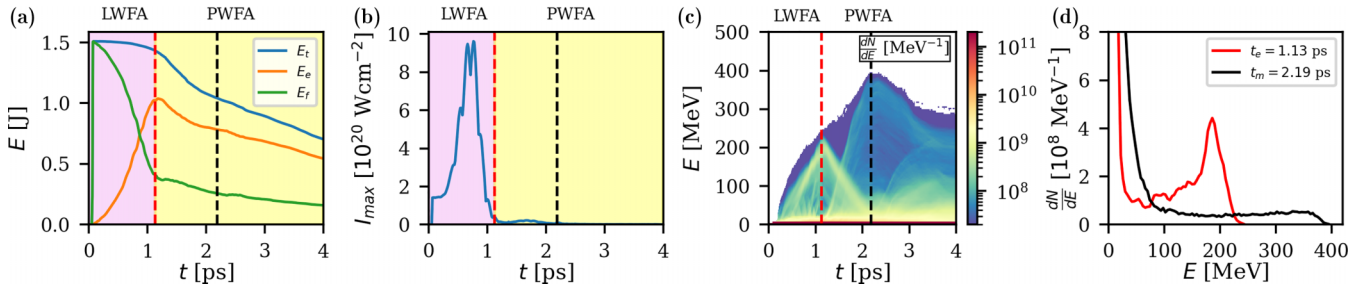

FIG. 2. (a) Temporal evolution of the total energy in the simulation box E_t (blue), the kinetic energy of simulated particles E_e (brown), electromagnetic energy E_f (green). (b) Temporal evolution of the quantity $I_{\max} = \max \frac{c\epsilon_0}{2}|\mathbf{E}|^2$. (c) Temporal evolution of electron spectra. (d) Electron spectra at the moments of the maximum conversion efficiency $E_e/E_{l,0}$ (red) and when the maximum electron energy is achieved (black).

box is achieved at the same moment the laser pulse vanishes ($t_e = 1.12$ ps). Its value is 1.01 J, corresponding to 67% of the initial laser energy. In the early phase ($t < t_e$), the total energy in the simulation box slowly decreases as the electrons not captured in the plasma wave gradually leave the simulation box, either through the transverse boundary, but mainly because of the movement of the simulation window. The later ($t > t_e$) more rapid decrease is caused by the transfer of the energy stored in the accelerated electron bunch to the wake wave driven by the bunch itself. The total electromagnetic energy is $E_f = 0.37$ J at $t = t_e$. It reasonably agrees with the theoretical expectation derived using a simple model of electrostatic fields in the relativistically moving ellipsoidal bubble. The electromagnetic energy stored in a bubble is defined as $U = \int_V (\frac{1}{2}\varepsilon\mathbf{E}^2 + \frac{1}{2\mu}\mathbf{B}^2)\mathrm{d}V \simeq \int_V (\frac{1}{2}\varepsilon E_x^2 + \frac{1}{2}\varepsilon E_r^2 + \frac{1}{2\mu}B_\theta^2)\mathrm{d}V$. The E_x, E_r, and B_θ fields within the bubble of the longitudinal and transverse semiaxes A and $B = C$ are given by a model from Ref. [38], generalizing the description of the fields in the spherical bubble [39,40]. After an integration, we obtain

$$U = \frac{8\pi}{15}\frac{q_e^2 n_e^2}{\varepsilon_0}\Phi_0^2\frac{A^2 + B^2}{A}, \tag{1}$$

where

$$\Phi_0 = \frac{3}{4}\frac{1}{\frac{1}{A^2} + \frac{1}{B^2} + \frac{1}{C^2}}. \tag{2}$$

For $A = B = C = R$, it simplifies to $U = \frac{\pi}{15}\frac{q_e^2}{\varepsilon_0}n_e^2 R^5$. Taking our values from simulations $n_e = 1.71 \times 10^{19}$ cm^{-3} and $A = 20\,\mu$m, $B = 12\,\mu$m, we get $U = 0.25$ J. Indeed, the energy stored in the wakefield itself is relatively large under such a configuration. Considering that the electron bunch has not yet achieved dephasing at the instant of t_e, the difference $1 - U/E_{l,0}$ sets the maximum energy fraction which can be transferred from the laser to the electrons, as, from that moment on, the energy accumulated in the bunch is consumed for driving its wakefield, potentially accelerating a fraction of trapped electrons to even higher energies, but losing the energy in total.

Indeed, such an evolution is illustrated in the electron spectra reported on panel (c). The initial energy peak, approximately 195 MeV, materializes at t_e. Subsequently, the electron bunch expends its energy amplifying an even more potent wakefield. A secondary electron bunch attains a maximum energy of 380 MeV at $t_m = 2.19$ ps. The vertical dashed lines, depicted across panels (a)–(c), delineate both those pivotal temporal junctures. Panel (d) presents the electron spectra at those two selected moments. At the time of t_e, the charge above [15, 100, 200] MeV is [6.3, 4.2, 0.95] nC.

A set of simulations was conducted to investigate the robustness of the scheme. Figure 3 presents the results of a parameter study. Scanning has been conducted in two directions. The plasma density is varied, and the laser focusing is either set to match the plasma density (left panels, $\frac{k_p w_0}{2\sqrt{a_0}} = 1$) or kept constant (right panels). Both injected charge Q [panels (a) and (b)] and laser-to-electron conversion efficiency $E_e/E_{l,0}$ [panels (c) and (d)] remain remarkably stable in the density region of 5×10^{18} cm^{-3} to 4×10^{19} cm^{-3}, reaching the values

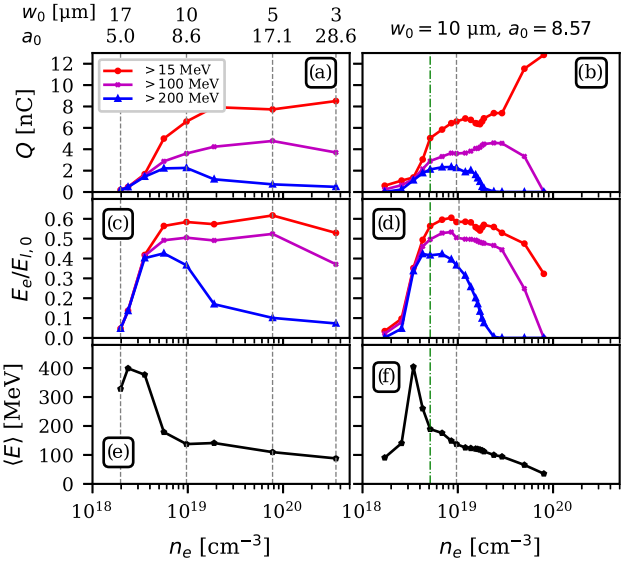

FIG. 3. Properties of the electron bunches when maximum conversion efficiency $E_e/E_{l,0}$ is achieved. (a), (b) Charge above [15, 100, 200] MeV (red circles, magenta crosses, blue triangles). (c), (d) $E_e/E_{l,0}$. (e), (f) Mean electron energy. (a), (c), (e) Laser focusing is matched to the plasma density ($\frac{k_p w_0}{2\sqrt{a_0}} = 1$), selected values of w_0 and a_0 are presented above the upper x-axis and marked with dashed gray lines. (b), (d), (f) Always kept $w_0 = 10\,\mu$m, $a_0 = 8.57$. A green dashed and dotted line and dashed gray line mark the matched density and the one chosen for the secondary sources example, respectively.

of about 5–7 nC and $\gtrsim$52%, respectively. The latter suggests that the saturation of $E_{e,>15\,\mathrm{MeV}}/E_{l,0}$ is achieved, considering the necessary losses to the electrostatic energy of the bubble.

Above the self-injection threshold, the mean energy of the accelerated electrons decreases [panels (e) and (f)] as the plasma density increases, in agreement with the scaling law [12]. Below such threshold, of about tens-of-pC bunches are accelerated in the following plasma wave buckets, achieving $E_e/E_{l,0}$ in order of percents at most. For the cases with $n_e > 5 \times 10^{19}$ cm^{-3} in the right column, we observe an increase of the injected charge up to 12.8 nC for $n_e = 8 \times 10^{19}$ cm^{-3}. There, the mixed LWFA/PWFA regime is entered even before the pump depletion of the driving pulse, resulting in the secondary injection to the bucket driven by the primary bunch, however, reducing the $E_e/E_{l,0}$ conversion efficiency significantly.

Reflecting the state of the art from the literature, a gradual progress toward the generation of higher-energy bunches achieved by the community can be observed. The selected experimental results with standard >25 fs, joule-class pulses [17–19,41–43] report charges in order of hundreds of pC for laser energies from 1.5 J [43] to 3.4 J [17]. In particular, the study [42] reports achieving charges above 100 MeV of 1.2, (1.7) nC with 27 fs laser pulse energies of 3, (10) J, respectively, and predicts a generation of 2.5 nC bunch with PW pulse of energy of 30 J. The conversion efficiency $E_e/E_{l,0}$ is always up to the order of percents. Similar efficiency has been achieved also with thin-film-compressed 13 fs, 3.2 J pulses [44]. The theoretical papers with 4.7 J [22] and 12 J [16], 30 fs pulses anticipate the conversion efficiency to electrons in order of 15%, in line with the analytical scaling based on similarity theory for $a_0 \gg 1$ [45] where $E_e/E_{l,0} \approx 0.2$ has been derived.

In recent years, the rapid advancements in high-repetition-rate, few-cycle laser systems [46] have spurred a growing interest in LWFA driven by mJ- and TW-level laser systems operating at up to kHz repetition rate. With 2–30 mJ laser energy, 1–50 MeV electron bunches of charge ranging from hundreds of fC to 25 pC are currently produced [47–49] or predicted [50–53]. Furthermore, 8 fs, 100 mJ pulses are expected to produce a laser-to-electrons conversion efficiency as high as 26% [54].

The newly available laser pulse parameters of short duration and large energy allow for a great laser to high energy electrons conversion efficiency in a broad range of plasma densities. The density itself then sets the final electron energy and charge. This new regime should make applications where both high number and high energy of accelerated electrons more and more pertinent, for example for very high energy electron radiotherapy (VHEE-RT) [55] or converted to secondary particles and radiation. Besides betatron radiation and inverse Compton scattering [56], the interaction of such energetic electron bunches with high-Z converters results in the emission of intense broadband x-ray radiation through a process of Bremsstrahlung [57,58] that can be converted to fast neutrons, promoting then applications such as nondestructive testing [59], industrial inspection [60] and imaging [61], or radiation therapy [62]. For example, in the case with $a_0 = 8.57$, $w_0 = 10\,\mu$m, and $n_e = 5.13 \times 10^{18}$ cm^{-3}, marked by a green dashed dotted line in Fig. 3, the Monte Carlo FLUKA [63,64] simulation suggests that Bremsstrahlung radiation carrying 27% of initial laser energy and 9.5×10^8 photoneutrons are released from the rear side of the 1.5 cm thick lead converted. The optimization of the secondary and tertiary sources of particles and radiation will be subjects of follow-up research.

In conclusion, we introduce a robust laser wakefield acceleration regime where the energy transfer efficiency from the laser pulse to relativistic electrons through the plasma wave is higher than 50%. It is characterized by an ultrarelativistic ($a_0 \gg 1$) and quasimatched ($k_p w_0 \approx 2\sqrt{a_0}$) pulse intensity so as to drive a plasma wave in the fully cavitated wakefield regime and by the short pulse duration ($\omega_p \tau_l \ll 1$) which favors a fast conversion of the laser pulse energy into the electromagnetic energy of the bubble. Combining both aspects results in significant self-steepening and self-focusing effects which reshape the laser pulse and induce massive and continuous self-injection. Moreover, the trapped electrons do not enter the dephasing phase of the acceleration process as the laser pulse energy is etched before. Our simulations confirm that with a few-cycle, joule-class laser pulses which are feasible with state-of-the-art technology based on the thin film compression technique, the electron bunches of charges of 11.5 nC above 15 MeV or 4.7 nC above 100 MeV can be generated, assuming the improvement in the focusability of such laser pulses.

This work was supported by the Extreme Light Infrastructure Nuclear Physics (ELI-NP) Phase II, a project cofinanced by the Romanian Government and the European Union through the European Regional Development Fund - the Competitiveness Operational Programme (1/07.07.2016, COP, ID 1334); the Romanian Ministry of Research and Innovation: PN23210105 (Phase 2, the Program Nucleu); SPARC and AMAP projects by IFA/ELI-RO_RDI; and the ELI-RO Grant Proiectul ELI12/16.10.2020 of the Romanian Government. We acknowledge EuroHPC Joint Undertaking for awarding us access to Karolina at IT4Innovations (VŠB-TU), Czechia under Projects No. EHPC-BEN-2023B05-023 and No. EHPC-REG-2023R02-006 (DD-23-83 and DD-23-157); Ministry of Education, Youth and Sports of the Czech Republic through the e-INFRA CZ (ID:90140); and CINECA HPC access through PRACE-ICEI standard call 2022 (P.I. Paolo Tomassini).

[1] E. Esarey, C. B. Schroeder, and W. P. Leemans, Physics of laser-driven plasma-based electron accelerators, Rev. Mod. Phys. **81**, 1229 (2009).

[2] V. Malka, J. Faure, Y. A. Gauduel, E. Lefebvre, A. Rousse, and K. T. Phuoc, Principles and applications of compact laser–plasma accelerators, Nat. Phys. **4**, 447 (2008).

[3] F. Albert and A. G. Thomas, Applications of laser wakefield accelerator-based light sources, Plasma Phys. Control. Fusion **58**, 103001 (2016).

[4] W. Sha, J.-C. Chanteloup, and G. Mourou, Ultrafast fiber technologies for compact laser wake field in medical application, in *Photonics* (MDPI, Basel, Switzerland, 2022), Vol. 9, p. 423.

[5] A. E. Hussein, N. Senabulya, Y. Ma, M. Streeter, B. Kettle, S. J. Dann, F. Albert, N. Bourgeois, S. Cipiccia, J. M. Cole *et al.*, Laser-wakefield accelerators for high-resolution x-ray imaging of complex microstructures, Sci. Rep. **9**, 3249 (2019).

[6] A. J. Gonsalves, K. Nakamura, J. Daniels, C. Benedetti, C. Pieronek, T. C. H. de Raadt, S. Steinke, J. H. Bin, S. S. Bulanov, J. Van Tilborg, C. G. R. Geddes, C. B. Schroeder, C. Toth, E. Esarey, K. Swanson, L. Fan-Chiang, G. Bagdasarov, N. Bobrova, V. Gasilov, G. Korn, P. Sasorov, and W. P. Leemans, Petawatt laser guiding and electron beam acceleration to 8 GeV in a laser-heated capillary discharge waveguide, Phys. Rev. Lett. **122**, 084801 (2019).

[7] C. Aniculaesei, T. Ha, S. Yoffe, L. Labun, S. Milton, E. McCary, M. M. Spinks, H. J. Quevedo, O. Z. Labun, R. Sain *et al.*, The acceleration of a high-charge electron bunch to 10 GeV in a 10-cm nanoparticle-assisted wakefield accelerator, Matter Radiat. Extremes **9**, 014001 (2024).

[8] C. Rechatin, J. Faure, A. Ben-Ismail, J. Lim, R. Fitour, A. Specka, H. Videau, A. Tafzi, F. Burgy, and V. Malka, Controlling the phase-space volume of injected electrons in a laser-plasma accelerator, Phys. Rev. Lett. **102**, 164801 (2009).

[9] L. T. Ke, K. Feng, W. T. Wang, Z. Y. Qin, C. H. Yu, Y. Wu, Y. Chen, R. Qi, Z. J. Zhang, Y. Xu, X. J. Yang, Y. X. Leng, J. S. Liu, R. X. Li, and Z. Z. Xu, Near-GeV electron beams at a few per-mille level from a laser wakefield accelerator via density-tailored plasma, Phys. Rev. Lett. **126**, 214801 (2021).

[10] E. Brunetti, R. P. Shanks, G. G. Manahan, M. R. Islam, B. Ersfeld, M. P. Anania, S. Cipiccia, R. C. Issac, G. Raj, G. Vieux, G. H. Welsh, S. M. Wiggins, and D. A. Jaroszynski, Low emittance, high brilliance relativistic electron beams from a laser-plasma accelerator, Phys. Rev. Lett. **105**, 215007 (2010).

[11] P. Tomassini, D. Terzani, L. Labate, G. Toci, A. Chance, Phu Anh Phi Nghiem, and L. A. Gizzi, High quality electron bunches for a multistage GeV accelerator with resonant multi-pulse ionization injection, Phys. Rev. Accel. Beams **22**, 111302 (2019).

[12] W. Lu, M. Tzoufras, C. Joshi, F. Tsung, W. Mori, J. Vieira, R. Fonseca, and L. Silva, Generating multi-GeV electron bunches using single stage laser wakefield acceleration in a 3D nonlinear regime, Phys. Rev. ST Accel. Beams **10**, 061301 (2007).

[13] S. P. Mangles, C. Murphy, Z. Najmudin, A. G. R. Thomas, J. Collier, A. E. Dangor, E. Divall, P. Foster, J. Gallacher, C. Hooker *et al.*, Monoenergetic beams of relativistic electrons from intense laser–plasma interactions, Nature (London) **431**, 535 (2004).

[14] C. Geddes, C. Toth, J. Van Tilborg, E. Esarey, C. Schroeder, D. Bruhwiler, C. Nieter, J. Cary, and W. Leemans, High-quality electron beams from a laser wakefield accelerator using plasma-channel guiding, Nature (London) **431**, 538 (2004).

[15] J. Faure, Y. Glinec, A. Pukhov, S. Kiselev, S. Gordienko, E. Lefebvre, J.-P. Rousseau, F. Burgy, and V. Malka, A laser–plasma accelerator producing monoenergetic electron beams, Nature (London) **431**, 541 (2004).

[16] A. Pukhov and J. Meyer-ter Vehn, Laser wake field acceleration: The highly non-linear broken-wave regime, Appl. Phys. B **74**, 355 (2002).

[17] Y. Li, D. Li, K. Huang, M. Tao, M. Li, J. Zhao, Y. Ma, X. Guo, J. Wang, M. Chen *et al.*, Generation of 20 Ka electron beam from a laser wakefield accelerator, Phys. Plasmas **24**, 023108 (2017).

[18] A. Döpp, L. Hehn, J. Götzfried, J. Wenz, M. Gilljohann, H. Ding, S. Schindler, F. Pfeiffer, and S. Karsch, Quick x-ray microtomography using a laser-driven betatron source, Optica **5**, 199 (2018).

[19] W. Schumaker, G. Sarri, M. Vargas, Z. Zhao, K. Behm, V. Chvykov, B. Dromey, B. Hou, A. Maksimchuk, J. Nees *et al.*, Measurements of high-energy radiation generation from laser-wakefield accelerated electron beams, Phys. Plasmas **21**, 056704 (2014).

[20] S. Bulanov, N. Naumova, F. Pegoraro, and J. Sakai, Particle injection into the wave acceleration phase due to nonlinear wake wave breaking, Phys. Rev. E **58**, R5257 (1998).

[21] P. Tomassini, M. Galimberti, A. Giulietti, D. Giulietti, L. Gizzi, L. Labate, and F. Pegoraro, Production of high-quality electron beams in numerical experiments of laser wakefield acceleration with longitudinal wave breaking, Phys. Rev. ST Accel. Beams **6**, 121301 (2003).

[22] M. G. Lobok, I. A. Andriyash, O. E. Vais, V. Malka, and V. Y. Bychenkov, Bright synchrotron radiation from relativistic self-trapping of a short laser pulse in near-critical density plasma, Phys. Rev. E **104**, L053201 (2021).

[23] G. Mourou, S. Mironov, E. Khazanov, and A. Sergeev, Single cycle thin film compressor opening the door to Zeptosecond-Exawatt physics, Eur. Phys. J.: Spec. Top. **223**, 1181 (2014).

[24] E. A. Khazanov, S. Y. Mironov, and G. Mourou, Nonlinear compression of high-power laser pulses: compression after compressor approach, Phys. Usp. **62**, 1096 (2019).

[25] J. I. Kim, Y. G. Kim, J. M. Yang, J. W. Yoon, J. H. Sung, S. K. Lee, and C. H. Nam, Sub-10 fs pulse generation by post-compression for peak-power enhancement of a 100-TW Ti: Sapphire laser, Opt. Express **30**, 8734 (2022).

[26] J. Wheeler, G. P. Bleotu, A. Naziru, R. Fabbri, M. Masruri, R. Secareanu, D. M. Farinella, G. Cojocaru, R. Ungureanu, E. Baynard *et al.*, Compressing high energy lasers through optical polymer films, in *Photonics* (MDPI, Basel, Switzerland, 2022), Vol. 9, p. 715.

[27] P.-G. Bleotu, J. Wheeler, S. Y. Mironov, V. Ginzburg, M. Masruri, A. Naziru, R. Secareanu, D. Ursescu, F. Perez, J. De Sousa *et al.*, Post-compression of high-energy, sub-picosecond laser pulses, High Power Laser Sci. Eng. **11**, e30 (2023).

[28] V. N. Ginzburg, I. V. Yakovlev, A. S. Zuev, A. P. Korobeynikova, A. A. Kochetkov, A. A. Kuz'min, S. Y. Mironov, A. Shaykin, I. A. Shaikin, and E. A. Khazanov, Compression after compressor: Threefold shortening of 200-TW laser pulses, Quantum Electron. **49**, 299 (2019).

[29] P.-G. Bleotu, J. Wheeler, D. Papadopoulos, M. Chabanis, J. Prudent, M. Frotin, L. Martin, N. Lebas, A. Freneaux, A. Beluze *et al.*, Spectral broadening for multi-Joule pulse compression in the APOLLON Long Focal Area facility, High Power Laser Sci. Eng. **10**, e9 (2022).

[30] V. Ginzburg, I. Yakovlev, A. Kochetkov, A. Kuzmin, S. Mironov, I. Shaikin, A. Shaykin, and E. Khazanov, 11 fs, 1.5 PW laser with nonlinear pulse compression, Opt. Express **29**, 28297 (2021).

[31] G. P. Bleotu, S. Popa, A.-M. Talposi, D. G. Matei, S. Roder, R. Ungureanu, J. Wheeler, G. Mourou, J. Fuchs, and D. Ursescu, Four cycles, focused post-compressed 100 TW laser pulses (unpublished).

[32] E. Esarey, C. B. Schroeder, B. A. Shadwick, J. S. Wurtele, and W. P. Leemans, Nonlinear theory of nonparaxial laser pulse propagation in plasma channels, Phys. Rev. Lett. **84**, 3081 (2000).

[33] J. Vieira, F. Fiúza, L. Silva, M. Tzoufras, and W. Mori, Onset of self-steepening of intense laser pulses in plasmas, New J. Phys. **12**, 045025 (2010).

[34] J. Derouillat, A. Beck, F. Pérez, T. Vinci, M. Chiaramello, A. Grassi, M. Flé, G. Bouchard, I. Plotnikov, N. Aunai *et al.*, SMILEI: A collaborative, open-source, multi-purpose particle-in-cell code for plasma simulation, Comput. Phys. Commun. **222**, 351 (2018).

[35] J. Huijts, I. A. Andriyash, L. Rovige, A. Vernier, and J. Faure, Identifying observable carrier-envelope phase effects in laser wakefield acceleration with near-single-cycle pulses, Phys. Plasmas **28**, 043101 (2021).

[36] See Supplemental Material at http://link.aps.org/supplemental/10.1103/PhysRevE.110.035202 for the list of presented simulations and their numerical parameters.

[37] B. Hidding, T. Königstein, J. Osterholz, S. Karsch, O. Willi, and G. Pretzler, Monoenergetic energy doubling in a hybrid laser-plasma wakefield accelerator, Phys. Rev. Lett. **104**, 195002 (2010).

[38] V. Horný, D. Mašlárová, V. Petržílka, O. Klimo, M. Kozlová, and M. Krůs, Optical injection dynamics in two laser wakefield acceleration configurations, Plasma Phys. Control. Fusion **60**, 064009 (2018).

[39] I. Kostyukov, A. Pukhov, and S. Kiselev, Phenomenological theory of laser-plasma interaction in "bubble" regime, Phys. Plasmas **11**, 5256 (2004).

[40] W. Lu, C. Huang, M. Zhou, M. Tzoufras, F. Tsung, W. Mori, and T. Katsouleas, A nonlinear theory for multidimensional relativistic plasma wave wakefields, Phys. Plasmas **13**, 056709 (2006).

[41] J. P. Couperus, R. Pausch, A. Köhler, O. Zarini, J. Krämer, M. Garten, A. Huebl, R. Gebhardt, U. Helbig, S. Bock *et al.*, Demonstration of a beam loaded nanocoulomb-class laser wakefield accelerator, Nat. Commun. **8**, 487 (2017).

[42] J. Götzfried, A. Döpp, M. F. Gilljohann, F. M. Foerster, H. Ding, S. Schindler, G. Schilling, A. Buck, L. Veisz, and S. Karsch, Physics of high-charge electron beams in laser-plasma wakefields, Phys. Rev. X **10**, 041015 (2020).

[43] J. Liu, H. Lu, H. Lu, H. Zhang, X. Wu, D. Wu, H. Lan, J. Zhang, J. Lv, Q. Ma *et al.*, Generation of ∼400 pC electron bunches in laser wakefield acceleration utilizing a structured plasma density profile, Phys. Plasmas **30**, 113103 (2023).

[44] S. Fourmaux, P. Lassonde, S. Y. Mironov, E. Hallin, F. Légaré, S. Maclean, E. Khazanov, G. Mourou, and J. Kieffer, Laser wakefield acceleration based x ray source using 225-TW and 13-fs laser pulses produced by thin film compression, Opt. Lett. **47**, 3163 (2022).

[45] S. Gordienko and A. Pukhov, Scalings for ultrarelativistic laser plasmas and quasimonoenergetic electrons, Phys. Plasmas **12**, 043109 (2005).

[46] J. Faure, D. Gustas, D. Guénot, A. Vernier, F. Böhle, M. Ouillé, S. Haessler, R. Lopez-Martens, and A. Lifschitz, A review of recent progress on laser-plasma acceleration at kHz repetition rate, Plasma Phys. Control. Fusion **61**, 014012 (2019).

[47] D. Guénot, D. Gustas, A. Vernier, B. Beaurepaire, F. Böhle, M. Bocoum, M. Lozano, A. Jullien, R. Lopez-Martens, A. Lifschitz *et al.*, Relativistic electron beams driven by kHz single-cycle light pulses, Nat. Photon. **11**, 293 (2017).

[48] C. Lazzarini, G. Grittani, P. Valenta, I. Zymak, R. Antipenkov, U. Chaulagain, L. Goncalves, A. Grenfell, M. Lamač, S. Lorenz *et al.*, Ultrarelativistic electron beams accelerated by terawatt scalable kHz laser, Phys. Plasmas **31**, 030703 (2024).

[49] D. Gustas, D. Guénot, A. Vernier, S. Dutt, F. Böhle, R. Lopez-Martens, A. Lifschitz, and J. Faure, High-charge relativistic electron bunches from a kHz laser-plasma accelerator, Phys. Rev. Accel. Beams **21**, 013401 (2018).

[50] G.-B. Zhang, M. Chen, D.-B. Zou, X.-Z. Zhu, B.-Y. Li, X.-H. Yang, F. Liu, T.-P. Yu, Y.-Y. Ma, and Z.-M. Sheng, Carrier-envelope-phase-controlled acceleration of multicolored attosecond electron bunches in a millijoule-laser-driven wakefield, Phys. Rev. Appl. **17**, 024051 (2022).

[51] X.-L. Zhu, W.-Y. Liu, M. Chen, S.-M. Weng, F. He, R. Assmann, Z.-M. Sheng, and J. Zhang, Generation of 100-MeV attosecond electron bunches with terawatt few-cycle laser pulses, Phys. Rev. Appl. **15**, 044039 (2021).

[52] J. Ferri, V. Horný, and T. Fülöp, Generation of attosecond electron bunches and x-ray pulses from few-cycle femtosecond laser pulses, Plasma Phys. Control. Fusion **63**, 045019 (2021).

[53] Z. Xiang, C. Yu, Z. Qin, X. Jiao, J. Cheng, Q. Zhou, G. Axi, J. Jie, Y. Huang, J. Cai *et al.*, Ultrahigh-brightness 50 MeV electron beam generation from laser wakefield acceleration in a weakly nonlinear regime, Matter Radiat. Extremes **9**, 035201 (2024).

[54] D. Papp, Z. Lécz, C. Kamperidis, and N. A. Hafz, Highly efficient few-cycle laser wakefield electron accelerator, Plasma Phys. Control. Fusion **63**, 065019 (2021).

[55] Y. Glinec, J. Faure, V. Malka, T. Fuchs, H. Szymanowski, and U. Oelfke, Radiotherapy with laser-plasma accelerators: Monte Carlo simulation of dose deposited by an experimental quasi-monoenergetic electron beam, Med. Phys. **33**, 155 (2006).

[56] S. Corde, K. Ta Phuoc, G. Lambert, R. Fitour, V. Malka, A. Rousse, A. Beck, and E. Lefebvre, Femtosecond x rays from laser-plasma accelerators, Rev. Mod. Phys. **85**, 1 (2013).

[57] Y. Glinec, J. Faure, L. Le Dain, S. Darbon, T. Hosokai, J. J. Santos, E. Lefebvre, J. P. Rousseau, F. Burgy, B. Mercier, and V. Malka, High-resolution γ-ray radiography produced by a laser-plasma driven electron source, Phys. Rev. Lett. **94**, 025003 (2005).

[58] S. Cipiccia, S. Wiggins, R. Shanks, M. Islam, G. Vieux, R. Issac, E. Brunetti, B. Ersfeld, G. H. Welsh, M. P. Anania *et al.*, A tuneable ultra-compact high-power, ultra-short pulsed, bright gamma-ray source based on bremsstrahlung radiation from laser-plasma accelerated electrons, J. Appl. Phys. **111**, 063302 (2012).

[59] Y. Wu, B. Zhu, G. Li, X. Zhang, M. Yu, K. Dong, T. Zhang, Y. Yang, B. Bi, J. Yang *et al.*, Towards high-energy, high-resolution computed tomography via a laser driven micro-spot gamma-ray source, Sci. Rep. **8**, 15888 (2018).

[60] C. Brenner, S. Mirfayzi, D. Rusby, C. Armstrong, A. Alejo, L. Wilson, R. Clarke, H. Ahmed, N. Butler, D. Haddock *et al.*, Laser-driven x-ray and neutron source development for industrial applications of plasma accelerators, Plasma Phys. Control. Fusion **58**, 014039 (2016).

[61] T. Brümmer, A. Debus, R. Pausch, J. Osterhoff, and F. Grüner, Design study for a compact laser-driven source for medical x-ray fluorescence imaging, Phys. Rev. Accel. Beams **23**, 031601 (2020).

[62] J. Alvarez, J. Fernández-Tobias, K. Mima, S. Nakai, S. Kar, Y. Kato, and J. Perlado, Laser driven neutron sources: Characteristics, applications and prospects, Phys. Procedia **60**, 29 (2014).

[63] T. Böhlen, F. Cerutti, M. Chin, A. Fassò, A. Ferrari, P. G. Ortega, A. Mairani, P. R. Sala, G. Smirnov, and V. Vlachoudis, The FLUKA code: Developments and challenges for high energy and medical applications, Nucl. Data Sheets **120**, 211 (2014).

[64] A. Fasso, A. Ferrari, J. Ranft, and P. R. Sala, FLUKA: A multi-particle transport code, Tech. Rep. (CERN-2005-10, 2005).